

Physiology of the Normal and Failing Heart

M. Chadi Alraies, Daniel J. Garry, and Mary G. Garry

Introduction – 22

The History of Cardiac Physiology – 22

Anatomical Structure of the Heart – 23

Blood Supply of the Heart – 25

Architectural Orientation of Cardiac Myofibers – 25

Histological Organization of the Adult Human Heart – 26

Innervation of the Heart – 27

The Role of Myoglobin – 28

Pressure Versus Volume – 30

Pressure–Volume Relationships – 31

Factors Affecting Pressure–Volume Loops – 32

Cardiac Preload – 32

Afterload – 34

Ventricular Contractility – 35

Ventricular Compliance – 35

Left Ventricular Remodeling and the Law of Laplace – 35

Summary – 35

References – 36

M.C. Alraies, MD, FACP
University of Minnesota, 420 Delaware Street SE, MMC 508, Minneapolis, MN 55455, USA
e-mail: alrai005@umn.edu

D.J. Garry, MD, PhD (✉)
Lillehei Heart Institute, Department of Medicine, University of Minnesota Medical Center,
University of Minnesota, 2231 6th Street SE, 4-146 Cancer and Cardiovascular Research Building,
Minneapolis, MN 55455, USA
e-mail: garry@umn.edu

M.G. Garry, PhD
Lillehei Heart Institute, Department of Medicine, University of Minnesota, 2231 6th Street SE, 4-147
Cancer and Cardiovascular Research Building, Minneapolis, MN 55455, USA
e-mail: garry002@umn.edu

Introduction

The adult human heart is an architecturally assembled organ that is a muscularized pump. This organ beats more than two billion times in a lifetime and delivers more than 1900 gallons of blood to every organ in the body each day. The coordinated activity of the respective chambers, vessels, and valves allows for immediate responses to the constant physiological demands and for the maintenance of homeostasis. As such, the heart is a dynamic and highly responsive organ. These physiological responses allow for an efficiently regulated cardiovascular system. The adult heart is capable of numerous adaptations, known as cardiac remodeling, that occur following injury or infarct. These adaptations are transiently beneficial and then become pathological. In this chapter, we outline the physiological response of the normal adult human heart. We also highlight the numerous adaptations of the failing heart which occur in an attempt to preserve cardiac output. Importantly, the adult human heart is a constantly changing organ that adapts to signals and cues that allow for performance—an organ that, even today, cannot be fully replaced by an engineered heart.

The History of Cardiac Physiology

The term “cardiac” is derived from the Greek word “kardia,” which means “related to the heart.” The history of cardiovascular physiology is richly decorated with discoveries and innovations. These historical advances provide an important platform for understanding the impact and mechanisms of emerging therapies for heart failure. Perhaps one of the earliest cardiovascular physiologists was William Harvey, MD (April 1, 1578 to June 3, 1657). In 1628, Dr. Harvey published his classic work on blood circulation, entitled *De Motu Cordis* (On the Motion of the Heart and Blood) [1]. In this publication, Dr. Harvey outlined the movement of blood via a circuit, the coordinated ventricular contractions, and the analysis of the vasculature. These observations emphasized the importance of the heart as a contractile pump as opposed to the more ancient view that the heart served as the source of the body’s heat (i.e., Galenic physiology). Dr. Harvey’s power of observation and discovery served as the basis for additional studies of the heart and blood vessels, which led to a detailed examination of the heart’s structure and function.

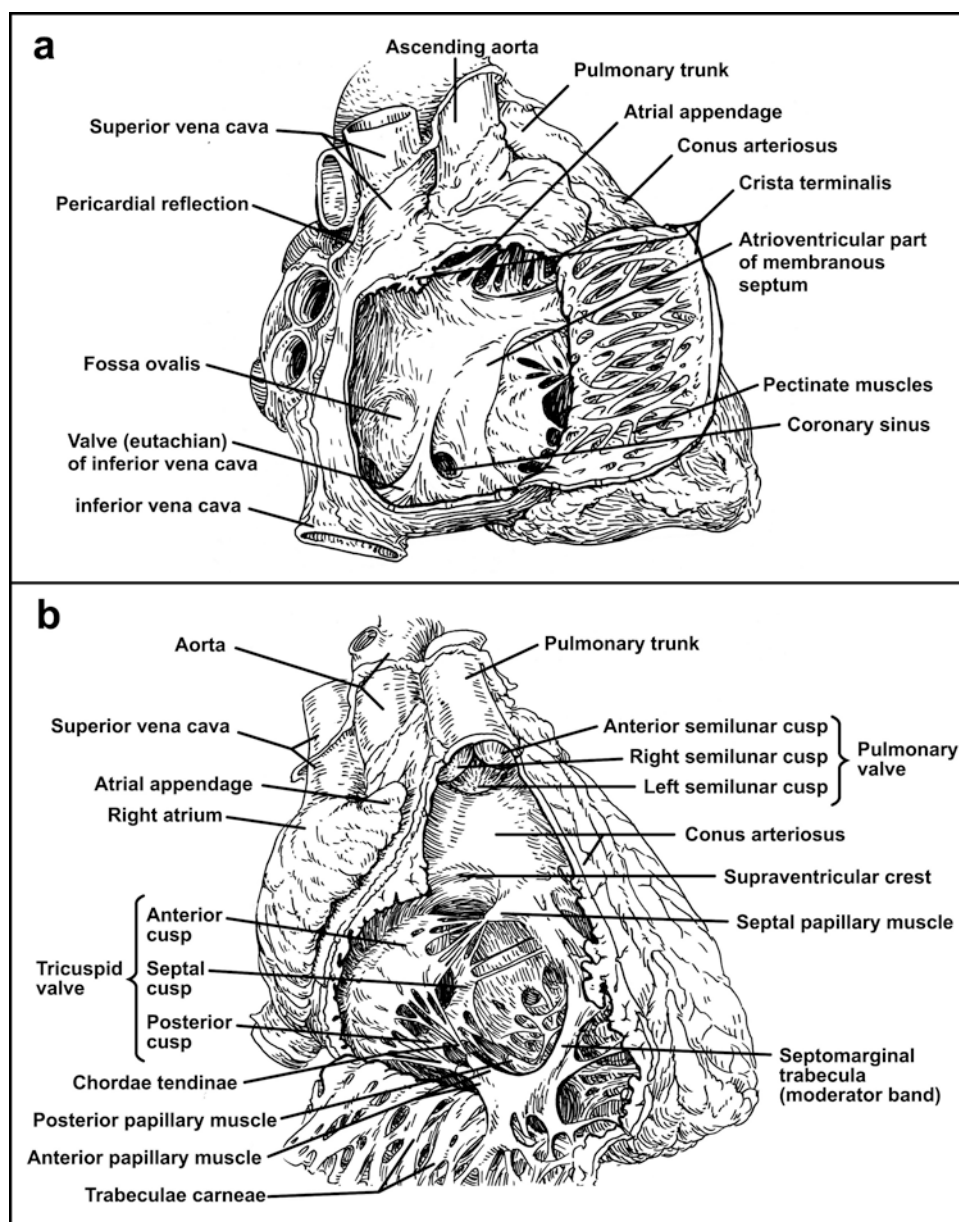
The importance of extracellular calcium in cardiac contraction had been appreciated since the classic studies in 1883 by Sydney Ringer, MD (1835–1910) (Ringer’s Lactate Solution) [2]. As outlined in these studies, Dr. Ringer established the importance of calcium, potassium, and sodium ions for the heart’s spontaneous contractile properties. In the ensuing years, Harold Reuter, MD, and N. Seitz, MD, discovered that a surface transport protein exchanged sodium for calcium in guinea pig atria [3]. Using an array of techniques, they found that the calcium sensitivity of the sarcomere and the regulation of calcium release from the sarcoplasmic reticulum could be studied in the absence of the sarcolemmal

barrier. Interest in regulating calcium removal from the cytosol was heightened when phospholamban (a micropeptide), an inhibitor protein associated with the heart, was discovered by Kirchberger, Tada, Katz, and Inui [4, 5]. In 1920, Carl J. Wiggers, MD, was the first to describe the simultaneous electrical and mechanical events of the cardiac cycle [6]. Preceding this discovery (1870), Adolph E. Fick, MD (September 3, 1829 to August 21, 1901), identified the relationship among oxygen consumption, arteriovenous oxygen difference, and total flow through the lungs that provided the means for the calculation of cardiac output (Fick principle) [7]. In the 1940s, Cournand and colleagues used atrial sampling and Fick’s principle to measure cardiac output in humans [8]. Otto Frank (June 21, 1865 to November 12, 1944) discovered that the maximum systolic pressure generated during isometric contraction was a function of the pre-systolic ventricular pressure (Frank–Starling law of the heart) [9]. In 1914, Ernest H. Starling (April 17, 1866 to May 2, 1927) showed that the ventricular stroke volume was a direct function of the end-diastolic volume (Frank–Starling law of the heart) [10]. In the mid-twentieth century, Stanley J. Sarnoff, MD (May 5, 1917 to May 25, 1990), demonstrated that stimulating the heart using inotropic agents could modulate the stroke work–preload relationship [11]. Similarly, Edmund H. Sonnenblick, MD (December 7, 1932 to September 22, 2007), used force–velocity relationships from isolated papillary muscle to quantify changes in contractility [12]. Dr. Sonnenblick showed that the maximum velocity of muscle shortening at zero afterload increased when positive inotropes such as norepinephrine were applied to the papillary muscle.

The interactions of the heart and blood vessels required to achieve cardiovascular homeostasis are complex and difficult to conceive and explore without the assistance of conceptual and mathematical models. In 1967, Arthur C. Guyton, MD (1919–2003), and Thomas D. Coleman, MD, proposed a model showing the integrated interactions of the heart, blood vessels, and kidney in the long-term regulation of arterial blood pressure [13]. The concept emphasized the kidney’s role as the main determinant of arterial pressure over the long term. Later, intrinsic and extrinsic regulation of blood flow in different vascular beds, baroreceptor and chemoreceptor reflexes, and hormonal influences was added to the basic renal-body fluid loop to help predict cardiovascular responses to different perturbations.

Several developments in the late twentieth century led to a shift in focus toward the cellular and molecular basis of cardiovascular functions. First, techniques for isolating and culturing cardiac and vascular cells were perfected. Second, advances in our understanding of cell signaling pathways provided a conceptual foundation for investigations of cardiac and vascular cell responses to specific disturbances of their physical and chemical environments. Third, new developments in light microscopy enabled optical monitoring of a wide variety of physiological variables in living cells in space and time. Finally, the revolution in molecular biology provided the tools to probe the impact

Fig. 2.1 The anatomical structures of the right side of the adult heart. **(a)** Schematic of the right atrium emphasizing the tricuspid valve, coronary sinus, and fossa ovalis. **(b)** Schematic of the right ventricle emphasizing the tricuspid valve, papillary muscles, thin ventricular wall, and outflow tract of the pulmonary artery



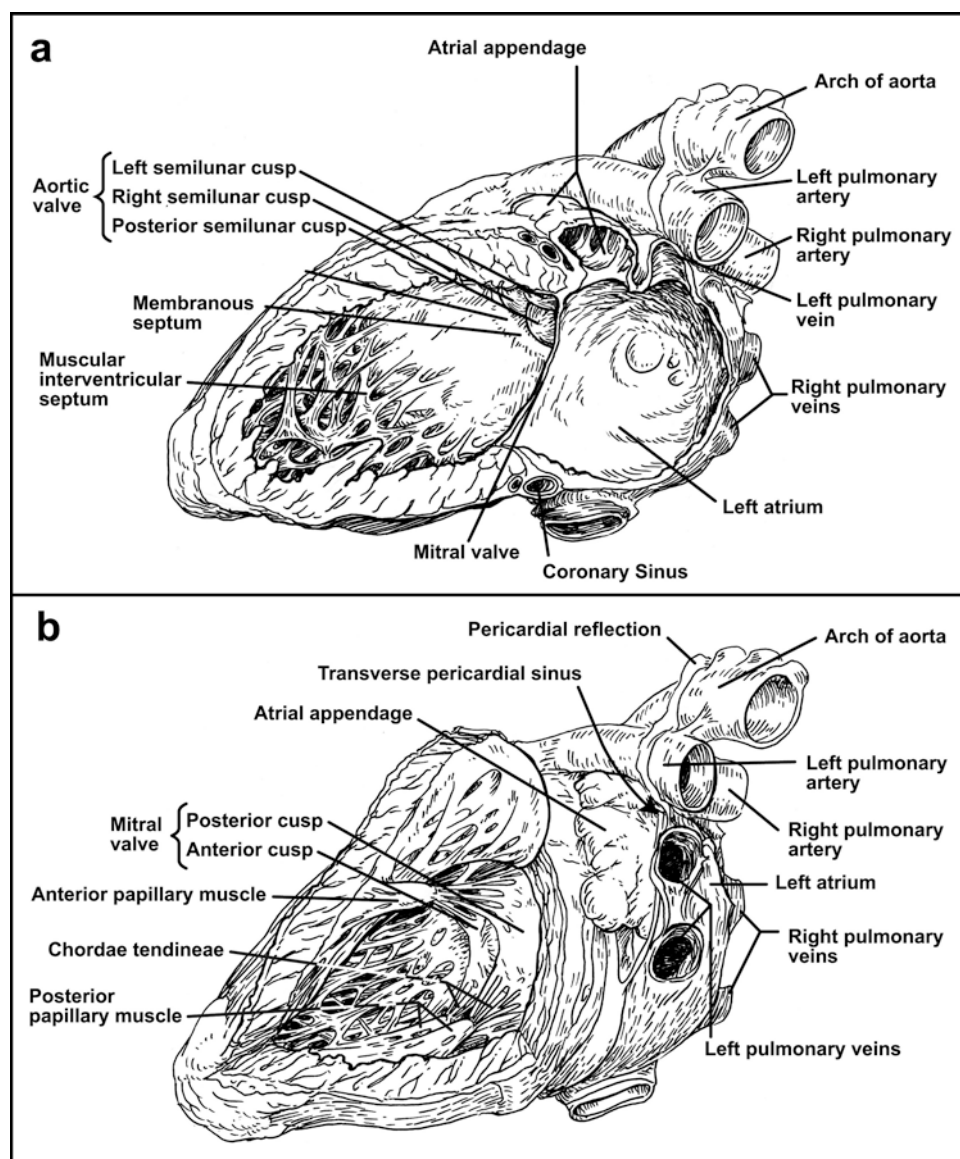
of gene overexpression, deletion, and modification on cultured cardiac and vascular cells and on the cardiovascular system of the intact animal. In recent decades, Eugene Braunwald, MD (b. 1929), a pioneer in the field of cardiovascular physiology, described studies in classic chapters of cardiovascular physiology, such as those addressing myocardial oxygen consumption, cardiovascular mechanics, and hemodynamics [14]. Dr. Braunwald illuminated our understanding of heart failure and revolutionized the management of postinfarction left ventricular remodeling.

Anatomical Structure of the Heart

Basic anatomical structure: The adult human heart is a four-chambered organ that weighs about 250–350 g. It is located within the mediastinum (T5–T8) and is closely associated

with the adjacent lungs. The heart is enclosed in the pericardial sac, which serves to position the heart in the chest as well as to limit its expansion. The heart's contractile or pumping action is due to the coordinated activity of myocardial muscle cells (cardiomyocytes), which execute the cardiac contraction–relaxation cycle to generate blood flow and pressure [15]. The normal left ventricular shape of the heart is comparable to a prolate ellipsoid with an inferior apical region and a superior base. The average adult heart is about 12 cm in length from base to apex [16]. The valves are nearly coplanar and essentially lie in the plane of the base of the heart (Fig. 2.1). Above the base are the great vessels (i.e., the ascending aorta and the main pulmonary artery) as well as the left and right atria. The pulmonary veins (left atrium), superior vena cava (right atrium), and inferior vena cava (right atrium) empty into the respective atria (Figs. 2.1 and 2.2).

Fig. 2.2 The anatomical structures of the left side of the adult heart. **(a)** Schematic of the left atrium emphasizing the pulmonary veins and mitral valve. **(b)** Schematic of the left ventricle emphasizing the thick myocardial wall, septum, mitral valve, papillary muscles (anterior and posterior papillary muscles), and aortic valve



The right atrium wall is paper thin and translucent between the pectinate muscles. It is subdivided into two parts: a posterior smooth-walled region that accommodates the entry of the blood from the superior and inferior venae cavae and the thin-walled trabeculated portion that constitutes the original embryonic right atrium (Fig. 2.1a,b). A ridge of muscle called the crista terminalis separates the two regions of the atrium (Fig. 2.1b) [17]. It is most prominent superiorly and is adjacent to the orifice of the superior vena cava (SVC). The superior portion of the right atrium is the right auricle, which is not well demarcated and consists of pectinate muscles. The anterior border of the ostium of the inferior vena cava (IVC) has a fold of tissue that forms the IVC valve or Eustachian valve, which is often visualized using echocardiography in the “normal” heart, but varies in size and may be absent. The coronary sinus enters the right atrium just anterior of the Eustachian valve and is often accessed during electrophysiology studies performed in an electrophysiology laboratory (Fig. 2.1b) [18]. The inter-

atrial septum forms the posteromedial wall of the right atrium. Although the interatrial septum is muscular, it has a shallow depression that forms the fossa ovalis. The area of the interatrial septum that is demarcated by the fossa ovalis, the right auricle, and the tricuspid valve is considered important in atrial pacing due to its proximity to the sinoatrial node. Furthermore, the fossa ovalis is often punctured during electrophysiology and interventional procedures to gain access to the left atrium (Fig. 2.1a).

The right ventricle (RV) is crescent or triangular in shape. A 3–5 mm-thick sheet of myocardial fibers forms the right ventricle. The RV has three segments: a posteroinferior inflow segment that contains the tricuspid valve, an anterosuperior outflow segment which is considered the origin of the pulmonary trunk, and the septum. Papillary muscle in the RV connects to the tricuspid valve via chordae tendineae, trabeculae carneae, and muscular bands (Fig. 2.1b). One of the muscular bands (moderator band) is often seen on echocardiogram. The tricuspid valve is anchored with several papillary muscles

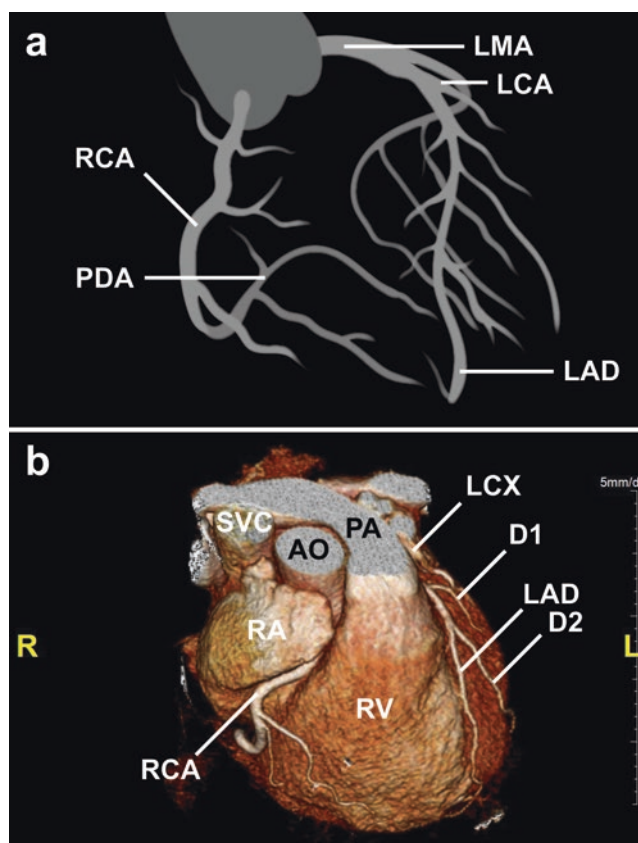
and their chordae tendineae (■ Fig. 2.1b). The pulmonary trunk arises superiorly from the RV and courses in a posterior–superior direction. The pulmonary trunk then bifurcates into the right and left pulmonary arteries (PAs).

The left ventricle (LV) is axisymmetric, truncated ellipsoid with almost 1 cm-thick muscular walls (■ Fig. 2.2a). This increased wall thickness is required in order to generate systemic pressures. In contrast, the left atrium (LA) is a thin, smooth-walled chamber that has four pulmonary veins entering from the right and left sides (■ Fig. 2.2a). The left atrial appendage (LAA) is variable in shape and size and is a continuation of the upper and anterior aspects of the LA. The LV septum is primarily muscular and consists of two layers: a thin layer on the RV and a thicker layer on the LV. The basilar portion of the ventricular septum is thinner and more fibrous and is referred to as the membranous septum.

The LAA contains small pectinate muscles and is considered the most common site for the development of thrombus, especially in patients with atrial fibrillation. The left ventricle (LV) has an average wall thickness of approximately three times that of the RV wall (■ Fig. 2.1a,b). The LV contains anterior and posterior papillary muscles, which connect to the mitral valve via the chordae tendineae and anchors the cusps to prevent prolapse or inversion (■ Fig. 2.2b).

Blood Supply of the Heart

The heart is a muscular organ and receives its blood supply from two main arteries: the left main coronary artery (LMA) and the right coronary artery (RCA) (■ Fig. 2.3a). The LM coronary artery originates from the left sinus of Valsalva and is short, 0.5–2 cm length and has a large diameter (3–4 mm). The LM coronary artery bifurcates into the left anterior descending (LAD) coronary artery and the left circumflex (LCx) artery (■ Fig. 2.3a, b) [19]. The LAD artery courses in the anterior interventricular groove and ascends a short distance following the posterior interventricular groove. The LAD artery has multiple branches including the septal branches, which supply the anterior two-thirds and apical portions of the septum, as well as a number of branches to the anteroapical portions of the left ventricle, including the anterior papillary muscle. The latter branches are called diagonals that vary in size and number. Usually, there are two or three diagonal vessels that are medium to large in size (1–2 mm diameter) (■ Fig. 2.3b). The second main branch from the LM coronary artery is the LCx coronary artery (■ Fig. 2.3b). It is usually smaller and courses in the left AV groove and branches into the obtuse marginal (OM1 and OM2) arteries to supply the upper lateral LV wall and the LA. The blood flow to the anterolateral papillary muscle in the LV is from the LAD (typically the diagonal branch) and the left circumflex (obtuse marginal artery) coronary arteries, and the blood flow to the posteromedial papillary muscle in the LV is from the posterior descending coronary artery (PDA), which is a branch of the RCA. This single source of blood supply contributes to posteromedial papillary muscle



■ **Fig. 2.3** The anatomy of the coronary vasculature in the adult heart. (a) Schematic demonstrating the coronary vasculature in the absence of the cellular components of the heart (Ao aorta, LM left main coronary artery, LAD left anterior descending coronary artery, LCX left circumflex coronary artery, RCA right coronary artery, PDA posterior descending coronary artery). (b) CT-angiography of the anterior aspect of the adult heart demonstrating the course of the RCA and LAD coronary vessels (LAD left anterior descending coronary artery, D1 first diagonal coronary artery, D2 second diagonal coronary artery, LCX left circumflex coronary artery, LV left ventricle, PA pulmonary artery, AO aorta, RA right atrium, RCA right coronary artery, RV right ventricle, SVC superior vena cava)

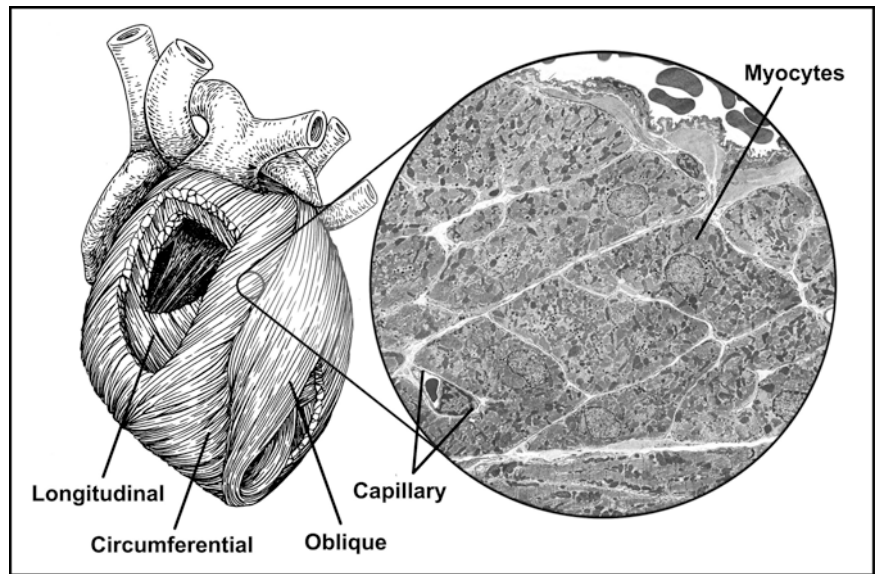
rupture and acute mitral regurgitation following right coronary artery occlusion [19, 20].

The right coronary artery (RCA) is the other main coronary artery that is responsible for the delivery of blood to the inferior wall of the heart (■ Fig. 2.3a). The RCA arises from the right coronary sinus of Valsalva of the aorta and courses in the right atrioventricular (AV) groove (■ Fig. 2.3b). The RCA branch, the posterior descending artery (PDA), courses in the posterior interventricular groove and supplies the posterior third of the interventricular septum [15].

Architectural Orientation of Cardiac Myofibers

The architecture of the heart is distinctive and functionally important. The myofibers are organized into laminated sheets that are approximately four cells thick. The ventricular

Fig. 2.4 Cellular and fiber orientations of the adult heart. Schematic of the adult heart demonstrating the oblique, circumferential, and longitudinal fiber orientations. Electron microscopic analysis of the cross section of the ventricular wall revealing mononuclear cardiomyocytes, myofibroblasts, endothelial cells, smooth muscle cells, and capillaries



myocardium is subdivided into three layers (superficial layer, middle layer, and deep layer) (■ Fig. 2.4) [15]. The superficial layer is composed of oblique fibers that form a sheet extending from the base and wrapping around the apex. These oblique fibers form a twin helix around the ventricle and cause a wringing effect (similar to wringing the water out of a towel) resulting in optimal ventricular filling and emptying. The middle layer consists of circumferential muscle bundles that are primarily located in the midwall at the base and closer to the epicardium [21]. The deep layer is composed of oblique, circumferential, and longitudinal fibers (■ Fig. 2.4). Collectively, the left ventricle has continuous fiber geometries with circumferential fibers associated with the upper septum and base and oblique fibers that extend from the midwall to the apex. This architecture of circumferential and oblique fibers results in increased efficiency of the pump (i.e., stress and strain) during the cardiac cycle.

Histological Organization of the Adult Human Heart

The myocardium comprises the vast majority of the heart's thickness (■ Fig. 2.4). It contains both myocytes and connective tissue (■ Fig. 2.4). Cardiac myocytes represent most of the myocardial mass and accounts for more than half the heart's weight [22]. About 70 % of the myocardium, however, is connective tissue that maintains the heart's strength and stiffness. Recently, flow cytometry studies in rodents suggested that the adult mouse heart contained 55 % myocytes and 45 % nonmyocytes, although investigators recognized the possibility of species differences regarding cellular composition. The nonmyocyte constituents include cells such as fibroblasts, myofibroblasts (smooth muscle-like fibroblasts), vascular smooth muscle, and endothelial cells (■ Fig. 2.4). Several types of myocytes are found in normal hearts, and they are classified based on their location in the atria and

ventricles [22, 23]. Atrial myocytes are smaller than ventricular myocytes. Ventricular myocytes are long and narrow in shape. They are approximately 20 μm in diameter, 60–120 μm in length, and have a volume of 15,000–45,000 μm^3 . Individual contractile myocytes in the atrium are elliptical in shape. The atrial myocytes are 5–6 μm in diameter, 20 μm in length, and have a volume of 500 μm^3 [24]. Compared to the ventricular myocytes, the atrial myocytes have bundles of atrial tissue separated by wide areas of collagen. Working myocytes are filled with cross-striated myofibers and mitochondria and usually contain a single centrally located nucleus (■ Figs. 2.4 and 2.5).

Atrial myocytes contain stores of active natriuretic peptide which functions as natriuretic factors and facilitates the dilation of vascular smooth muscle. The increasing stretch of the cardiac wall caused by vascular congestion with decompensated heart failure is a potent stimulus for the release of these peptides from the atria and ventricles. Cardiomyocytes contain a large number of myofilaments that are organized in a regular array of cross striations (■ Fig. 2.5). The cross striations of the myocardium reflect the organization of the contractile proteins into thick and thin filaments [22]. The sarcomere is defined as the area between the two Z lines and is considered the fundamental unit of striated muscle (■ Fig. 2.5).

As schematized in ■ Fig. 2.5, the sarcomere contains the central A band and the two adjacent I bands. The sarcomere consists of the thick filaments composed largely of myosin that extend the length of the A band and contribute to the dark staining characteristics and its high birefringence. The thin filaments are composed of actin and the associated regulatory proteins—tropomyosin and troponin. Together, they form a complex that extends the length of the I bands and are characterized by the lightly stained striations and decreased birefringence. A broad dense M band is located in the center of each A band, while the I bands are bisected by Z lines (■ Fig. 2.5).

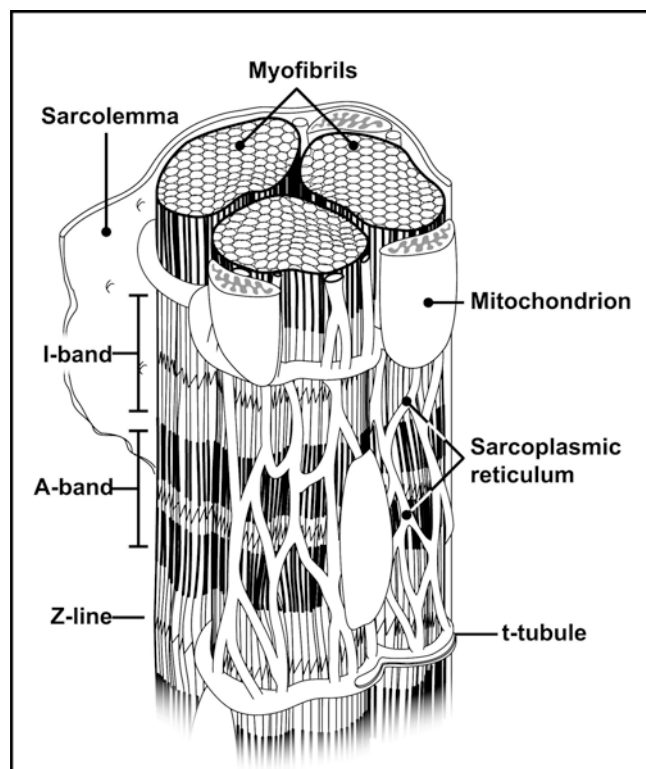


Fig. 2.5 Schematic of the organelles and cellular components associated with the cardiomyocyte. Note the overlying sarcolemma, ATP-producing mitochondria, sarcoplasmic reticulum, and t-tubule network. The sarcomere is defined by the Z lines and consists of myosin heavy chains (*thick filaments*) and actin chains (*thin filaments*). The A band consists of both the *thick* and *thin* filaments, whereas the I band consists of only the *thin* filaments

Innervation of the Heart

The parasympathetic (cholinergic) and sympathetic (adren-ergic) nerve fibers innervate the heart. The parasympathetic fibers arise from the cardiac components of the cranial neural crest cells and are propagated to the heart via the vagus nerve (■ Fig. 2.6). The vagus nerve is a mixed nerve that has both sensory and motor nerves. The right and the left vagal nerves course from the medulla to the heart via the carotid sheath and primarily innervate the sinoatrial (SA) and AV nodes.

The sympathetic nerve fibers arise from the medulla and course to the heart from the sympathetic ganglia (■ Fig. 2.6). The sensory nerves arise from the ectodermal placode of the nodose ganglion and are propagated via the vagus nerve. The nucleus ambiguus, the nucleus solitarius, and the dorsal motor nucleus in the medulla provide autonomic neuronal control for the cardiovascular system via the vagus nerve and the sympathetic ganglia. The nucleus solitarius receives sensory afferent input from chemoreceptors and baroreceptors and is a control center for the baroreflex (as well as exercise-induced reflexes such as the exercise pressor reflex and central command). The nucleus ambiguus and the dorsomedial nucleus (DMN) provide parasympathetic control for the parasympathetic control for the heart.

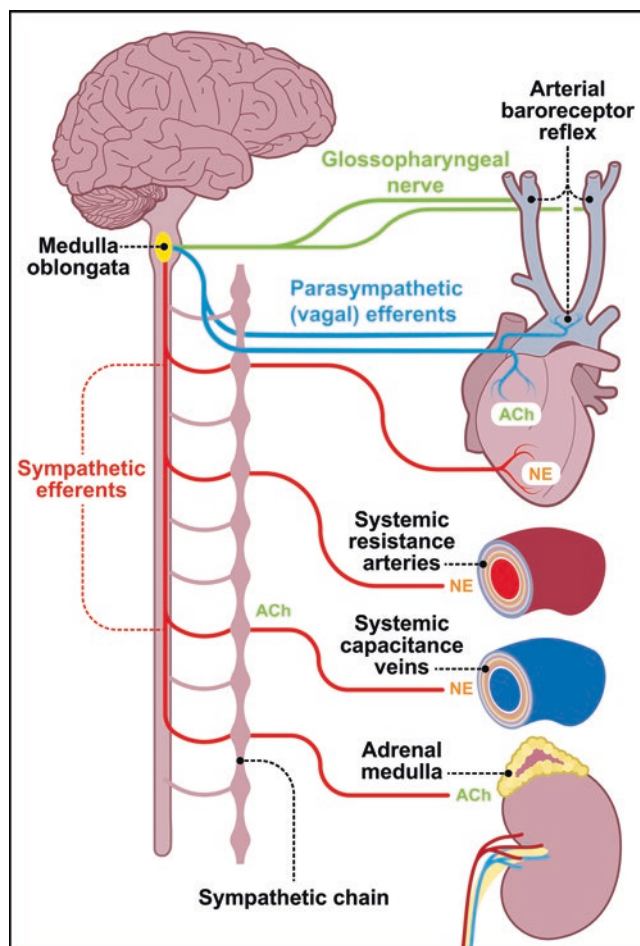


Fig. 2.6 Autonomic nervous system and the regulation of the cardiovascular system. Parasympathetic (ACh) and sympathetic (NE) innervation from the medulla oblongata to the cardiovascular target organs such as the arterial baroreceptor, atria, ventricles, vasculature, and adrenal glands, resulting in a coordinated response during rest or stress. Note the parasympathetic (ACh acetylcholine) and sympathetic (NE norepinephrine) neurotransmitters

Sympathetic efferent nerves originate from the cervical and thoracic sympathetic ganglia and course with the blood vessels to innervate the atria and ventricles. The effects of the sympathetic nervous system are mediated by norepinephrine that binds to alpha-adrenoreceptors (to regulate vasoconstriction of the vasculature in response to dehydration) or beta-1 adrenoreceptors to increase chronotropy, lusitropy, inotropy, and conduction velocity. The parasympathetic system mediates its effects by the release of acetylcholine, which binds muscarinic receptors and regulates the SA and AV nodes (■ Fig. 2.6).

Collectively, the cardiovascular innervation and its global impact on the cardiac output are evident in a number of reflexes (i.e., vasovagal syncope, Bezold-Jarisch reflex, Valsalva maneuver, carotid sinus reflex, etc.). In the failing heart, decreased cardiac output promotes an increase in sympathetic activity resulting in remodeling and is associated with increased arrhythmias and sudden cardiac death. Heart failure symptoms and progression of disease are exacerbated

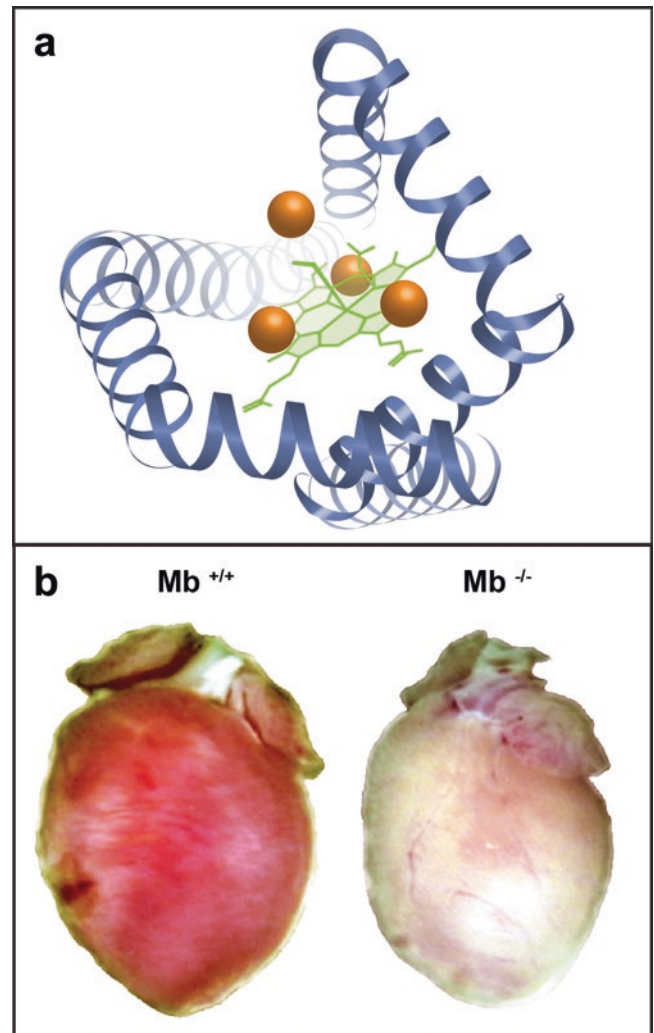
by a hyperadrenergic state. This increase in the sympathetic nervous system results in tachycardia, vasoconstriction, increased afterload, diaphoresis, oliguria, increased myocardial oxygen consumption, and progressive left ventricular remodeling. In short, norepinephrine becomes toxic to the myocardium. In patients with advanced heart failure who receive a cardiac transplant, the graft is denervated (i.e., vagus nerves are severed), and, typically, the heart rate is about 105 bpm.

The Role of Myoglobin

Tissue hemoglobins are found in diverse organisms including plants, mollusks, and mammals. These tissue hemoglobins include cytoglobin, neuroglobin, and myoglobin [4, 25]. In vertebrates, myoglobin is restricted to striated muscle (cardiomyocytes and oxidative skeletal myofibers) and is a monomeric cytoplasmic hemoprotein consisting of 154 amino acids [26, 27]. Myoglobin is named because of its functional and structural similarity to hemoglobin. Evolutionarily, myoglobin and hemoglobin arose from a common ancestral gene more than 500 million years ago [26, 28, 29]. In 1958, myoglobin was the first protein to be subjected to definitive structural analysis (■ Fig. 2.7a) [30]. Subsequently, a number of studies have established that the structure of myoglobin consists of a heme pocket, which is bracketed by histidine residues and has a backbone of eight α -helices (■ Fig. 2.7a). The flanking histidine residues stabilize the heme group and allow for the concentration of ligands (e.g., dioxygen, nitric oxide, carbon monoxide, etc.) to bind to the heme residue of myoglobin (■ Fig. 2.7a). In this fashion, myoglobin has been shown to have important roles as a facilitator of oxygen transport to mitochondria to maintain oxidative phosphorylation (and the generation of adenosine 5'-triphosphate, ATP) for myocardial contractility, as well as serve as a modulator of nitric oxide (NO) bioavailability and as a scavenger of reactive oxygen species [27, 31].

Previous studies using gene disruption technologies engineered a mouse model that lacked myoglobin (■ Fig. 2.7b) [32]. While many mutant embryos were nonviable, viable myoglobin null mice had preserved cardiac performance due to a number of adaptive mechanisms including an induction of the hypoxia-inducible molecular program, neovascularogenesis, and increased coronary flow [25, 33]. Collectively, the results of these genetic studies underscore the importance of myoglobin (and its role in oxygen transport and the generation of ATP), the redundancy of other tissue hemoglobins (in the absence of myoglobin), and the role of adaptive mechanisms to promote cardiac function, even in the absence of myoglobin [32].

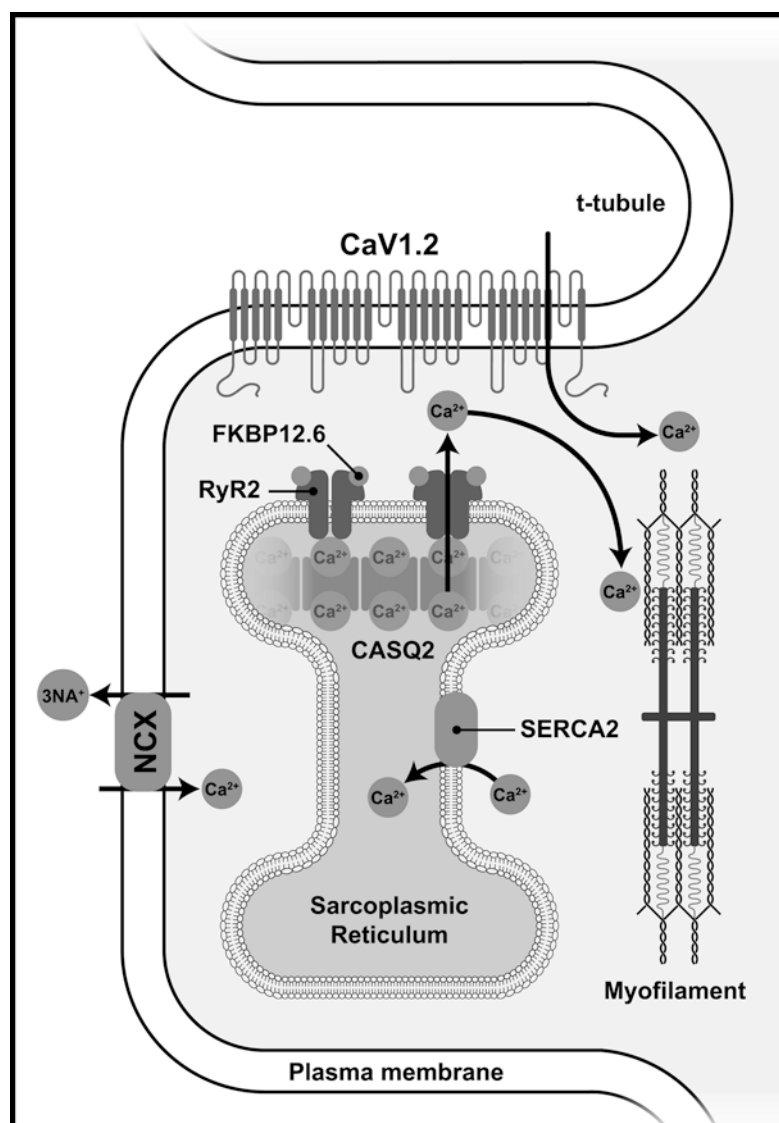
Cardiac contraction and relaxation: The contractile proteins of the heart—actin and myosin—lie within the cardiomyocytes, which constitute about 75 % of the total volume of the myocardium (■ Fig. 2.5) [34]. The physical interactions between myosin and actin are activated by calcium and regulated by tropomyosin and troponins (■ Fig. 2.8) [22, 28].



■ **Fig. 2.7** Myoglobin is an essential hemoprotein for oxygen delivery to the cardiomyocyte. (a) Myoglobin was the first protein to have its structure defined. It contains a heme pocket stabilized by histidine residues that promotes the binding of dioxygen, nitric oxide, and carbon monoxide. (b) Using a gene disruption strategy, mice lacking myoglobin were engineered. The functional importance of myoglobin was evident as mice lacking myoglobin were viable only as a result of an increase in the hypoxia-inducible molecular program (Hif1), resulting in an increase in other tissue hemoglobins and myocardial vasculature

Troponins have several subtypes (C, I, and T) and are associated with actin thin filaments. The signaling process that initiates cardiac systole, called excitation–contraction (EC) coupling, begins when an action potential depolarizes the plasma membrane [35]. This EC coupling opens L-type voltage-dependent calcium channels during the action potential plateau and allows an influx of calcium to enter the cytosol from the extracellular fluid (■ Fig. 2.8) [22, 36]. This calcium influx triggers the opening of calcium-release channels in the sarcoplasmic reticulum (via the ryanodine receptor 2, RyR2) that releases a larger pool of this activator to the cytosol from stores within this intracellular membrane system (■ Fig. 2.8) [5, 37]. This increased cytosolic calcium concentration facilitates the binding of calcium to troponin C and the induction of contraction [38, 39]. Following

Fig. 2.8 Calcium signaling regulates myofilament contractility. Schematic highlighting the calcium influx into the cytosol of the cardiomyocyte, which promotes the release of calcium from the sarcoplasmic reticulum stores via the RYR2 channel. Calcium then binds to the myofilament unit and promotes contraction (systole). Calcium is then transported back into the SR via SERCA2 to promote diastole (*CaV1.2* voltage-dependent L-type α -1C subunit calcium channel, *FKBP12.6* FK506 binding protein 12.6 that interacts with *RyR2*, *RyR2* ryanodine receptor2, *SERCA2* sarcoplasmic endoplasmic reticulum calcium ATPase, *CASQ2* calsequestrin 2, *NCX* sodium/calcium exchanger, *NA* sodium, *Ca*, calcium)



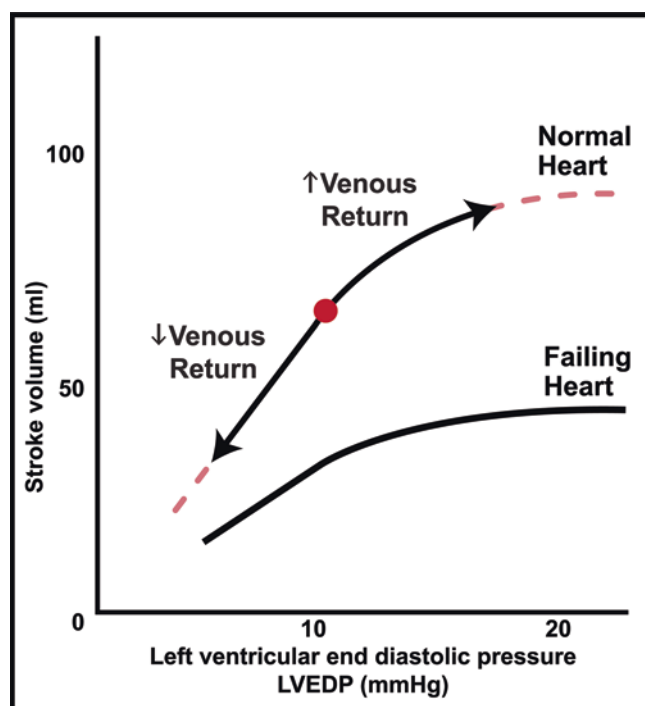
contraction, the calcium is released from troponin C, and reuptake into the SR is facilitated by the SR calcium-ATPase 2a (SERCA2a) calcium pump (Fig. 2.8). The heart relaxes when calcium is transported out of the cytosol. A smaller amount of calcium is transported from the cytosol into the extracellular space by a plasma membrane calcium pump and sodium/calcium exchanger [22, 36]. The total time period required for cardiomyocyte depolarization, calcium-induced calcium release, contraction, relaxation, and recovery in the adult human heart is about 600 msec [38].

Regulation of cardiac contractile performance: Two mechanisms are traditionally viewed as essential for the regulation of the heart's contractile performance: the length-dependent regulation (the Frank–Starling law of the heart) and inotropic/lusitropic properties (Fig. 2.9).

End-diastolic volume: the Frank–Starling mechanism: The length-dependent regulation (Starling's law of the heart) is due to variations in end-diastolic volume that results in

changes in sarcomere length and impacts the stroke volume of the heart (Fig. 2.9) [10]. This mechanism functions in matching the heart's output during systole to the return of blood during diastole [40]. Starling's law (or the Frank–Starling mechanism) showed that the greater the volume of the heart in diastole [(end-diastolic volume, EDV, which would increase the filling pressures; end-diastolic pressure, EDP)], the more forceful the contraction, which would increase the stroke volume (SV) [41]. Conversely, decreasing venous return is associated with decreased EDP and decreased SV (Fig. 2.9).

Regulation by inotropic properties: Changes in myocardial contractility are an important feature of cardiac muscle. Inotrope or myocardial contractility is the manifestation of all the factors that influence the interactions between contractile proteins with the exception of those that impact preload and afterload [13, 24]. Myocardial contractility occurs when the ability of the myocardium to do work is modified by factors other than altered fiber length (Starling's law). Myocardial



■ Fig. 2.9 Regulatory mechanisms that impact cardiac output. Frank–Starling curve demonstrating increased stroke volume in response to increased venous return to the heart resulting in increased cardiac output. Note the Frank–Starling curve in the failing heart with decreased stroke volume at any LVEDP

contractility is the heart's ejection and/or pressure development when the preload (venous return—EDV) and afterload (arterial pressure) are held constant. Most of the rapidly occurring changes in myocardial contractility are facilitated by variations in the amount of calcium delivered to the contractile proteins during excitation–contraction coupling [15, 21, 42].

Regulation by lusitropic (relaxation) properties: The clinical importance and quantification of the lusitropic property of the myocardium was not fully appreciated until echocardiography and nuclear techniques were developed. These techniques are able to measure the changes in the rate and the degree of ventricular filling and afford the opportunity to examine diastolic function in adult human patients [42, 43]. The heart relaxes when energy-dependent calcium pumps and exchangers lower cytosolic calcium concentration, which promotes the dissociation of calcium from troponin C. Relaxation is not simply the reversal of the processes involved in excitation–contraction coupling, because different mechanisms participate in calcium release and removal from the cytosol.

The cardiac cycle: The cardiac cycle is divided into systole and diastole (■ Fig. 2.10). These are further subdivided into four phases: isovolumetric contraction, ejection, isovolumetric relaxation, and filling (■ Fig. 2.10). The relationship between ventricular pressure and volume during the cardiac cycle can be illustrated by pressure–volume loops that will be discussed later in this chapter [6, 44].

The cardiac cycle consists of diastolic ventricular filling and augmentation by atrial systole to achieve the end-diastolic volume. During this period, the LV pressure increases until it exceeds that in the left atrium (normally 10–15 mmHg), which promotes the closure of the atrioventricular valves (i.e., the mitral and tricuspid valves) (■ Fig. 2.11). Following the closure of the AV valves, the LV and RV volume cannot change, and contraction must be isovolumetric (isovolumetric contraction) until the aortic (and pulmonary) valve(s) is forced open as the ventricular pressure exceeds that in the aorta and pulmonary artery (■ Figs. 2.10 and 2.11). Once the aortic (and pulmonary) valves are opened, blood is ejected from the ventricles into the major vessels, which is the phase of maximal ejection. The speed of ejection of blood is determined both by the pressure gradient across the aortic valve and by the elastic properties of the aorta, which undergoes systolic expansion (■ Fig. 2.12). Meanwhile, atrial pressure progressively increases during ventricular systole as blood continues to enter the atrium while the atrioventricular (AV) valves are closed. Once the ventricle reaches its end-systolic volume (ESV), there is a period of isovolumetric relaxation, which promotes the opening of the AV valves (mitral and tricuspid) and diastolic filling from the atrium into the ventricle to begin the next cycle (■ Figs. 2.10 and 2.11).

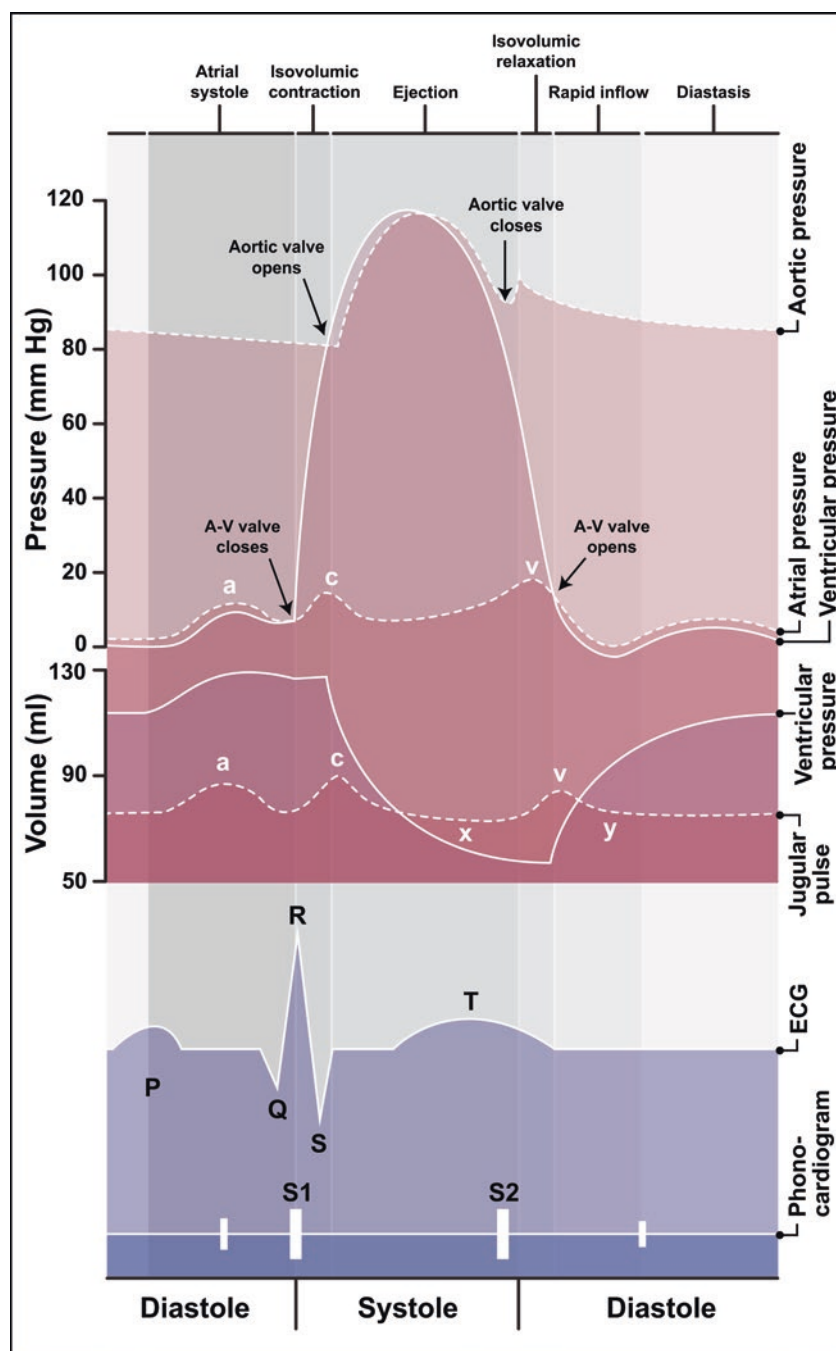
Throughout the diastolic ventricular filling period, the pressure gradient between the atrium and ventricle is minimal. This happens because a normal open mitral or tricuspid valve offers little resistance to flow; there is also significant passive filling of both the atrium and ventricle as blood returns from the systemic or pulmonary venous system. At a normal resting heart rate, diastole occupies about two-thirds of the cardiac cycle (■ Fig. 2.10). With increased heart rate, both systolic and diastolic intervals will shorten. Systole is defined by the interval between the first and second heart sounds lasting from the first heart sound to the point of closure of the aortic valve (■ Fig. 2.10). The remainder of the cardiac cycle is diastole.

The main difference between the left and right pumping systems is the pressure magnitude. In the normal heart, the pressures developed in the right heart are significantly lower than those on the left side, because resistance across the pulmonary vasculature is far less than the resistance to flow offered by the systemic vascular system. Normal pulmonary artery systolic and diastolic pressures typically do not exceed 30 mmHg and 15 mmHg respectively; maximal right atrial pressure is generally 8 mmHg (■ Fig. 2.10).

Pressure Versus Volume

Contractility is the inherent capacity of the myocardium to contract independently of the changes in the preload or afterload. Increased contractility means a greater rate of contraction, to reach a greater peak force. Frequently, increased contractility is associated with enhanced rates of relaxation, called the lusitropic effect (■ Fig. 2.11). An alternative term for contractility is inotropy. Contractility is an important regulator of the myocardial oxygen uptake. Factors that increase contractility include adrenergic stimulation, temperature, redox state, and pH.

Fig. 2.10 Hemodynamic and physical exam signs associated with the cardiac cycle. Overlapping depiction highlighting the phases of the cardiac cycle; hemodynamics associated with the aorta, left ventricle, and atria; and electrocardiogram. (P wave represents atrial depolarization, QRS represents ventricular depolarization, and T wave represents repolarization.) Note S1 corresponds to the closure of the atrioventricular valves (tricuspid and mitral valves), and S2 corresponds to the closure of the semilunar valves (aortic and pulmonic valves). Individual hemodynamic tracings emphasize that the jugular venous pressure tracing reflects atrial contraction (*a*-wave), ventricular contraction, and bulging of the tricuspid valve into the right atrium during isovolumetric systole (*c*-wave), atrial venous filling (*v*-wave), atrial relaxation and downward movement of the tricuspid valve (*x*-descent), and the filling of the ventricle following the opening of the tricuspid valve (*y*-descent)



Pressure–Volume Relationships

Measurements using pressure–volume loops (PVLs) are traditionally used to assess the contractile behavior of the intact heart. The relationship between ventricular pressure and volume during the cardiac cycle has been described using pressure–volume loops. The relationship can be demonstrated by plotting LV pressure versus LV volume through one complete cardiac cycle (■ Fig. 2.11) [41, 45].

As illustrated in ■ Fig. 2.11, the cycle starts with the opening of the mitral valve (A), which allows blood to flow from the atrium into the ventricle during the filling phase (A–B). Systole, then, is initiated at a point along the end-

diastolic pressure–volume relationship (end diastole) located at the lower right corner of the loop (B), which is associated with the closure of the mitral valve. Once the mitral valve closes, the intraventricular pressure increases rapidly while both the mitral and aortic valves are closed. This phase represents isovolumetric contraction (IVC) (B–C). As soon as the aortic valve opens, the ventricle is exposed to the aortic pressure (C), and the ejection phase begins (C–D). Systole ends when the ventricular pressure and volume reach the end-systolic pressure–volume relationship, which describes the inotropic state of the ventricle at which the aortic valve closes (D). When the aortic valve closes (D), the blood is constrained within the ventricle; as a

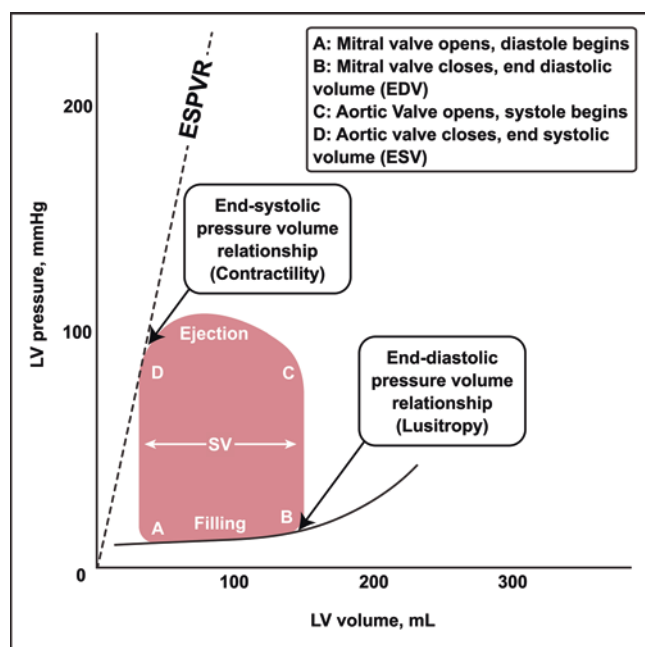


Fig. 2.11 Pressure-volume relationship of the adult heart. Note the pressure-volume relationship of the functional adult heart (ESPVR end-systolic pressure-volume relationship, EDV end-diastolic volume, ESV end-systolic volume, SV stroke volume, LV left ventricular)

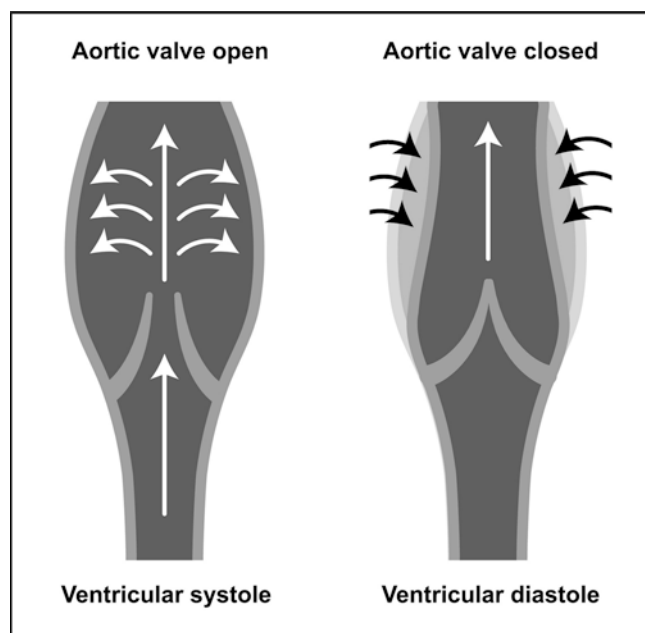


Fig. 2.12 The aorta is a compliant vessel. Schematic of the compliance of the aorta during systole and diastole. Note that this compliance decreases significantly with age and disease

result, relaxation begins. This phase is referred to as the iso-volumetric relaxation (IVR) (D-A). When the LV pressure falls below that in the left atrium, the mitral valve opens (A) and blood flows from the atrium into the ventricle during the filling phase (A-B). Therefore, systole begins at (B) and ends at (D), while ejection begins at (C) and ends at (D). Similarly, diastole begins at (D) and ends at (B), while filling begins at (A) and ends at (B) (Fig. 2.11).

Factors Affecting Pressure-Volume Loops

The major determinants of the left ventricular pressure-volume relationship and cardiac output are cardiac preload (ventricular volume), myocardial contractility (inotropy), and afterload (Table 2.1) (Fig. 2.13). Unlike other striated muscles such as skeletal muscle, the myocardial PVL is constrained within two pressure-volume factors. The first factor is the end-systolic pressure-volume relationship, which is mainly determined by the inotropic property of the contracting myocardium. The second factor is the end-diastolic pressure-volume relationship, which is determined by the lusitropic property of the relaxed myocardium. Ventricular end-diastolic volume (EDV) is determined by the venous return, end-systolic volume and the lusitropic properties of the ventricle. Conversely, end-systolic volume is determined by EDV, aortic impedance, and contractility. These ventricular changes can be complex as preload, afterload, and inotropy are interdependent variables (Fig. 2.13a, b, d). The interdependency refers to the changing of one variable impact and changes the other variables as well.

Cardiac Preload

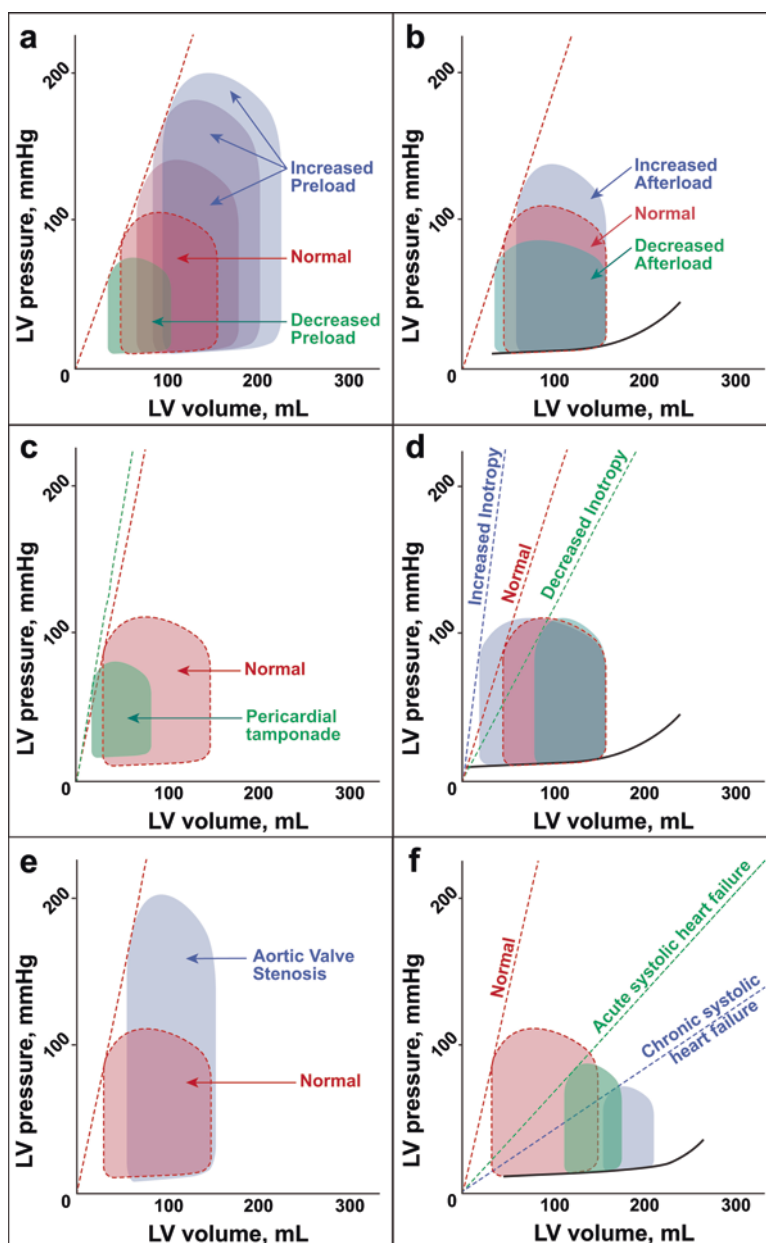
Cardiac preload is a semiquantitative composite assessment that is described as end-diastolic myocardial fiber tension, end-diastolic myocardial fiber length, ventricular end-diastolic volume, and ventricular end-diastolic filling pressure (Table 2.1) (Fig. 2.13a). Cardiac preload is an assessment of end-diastolic pressure—the ventricular pressure measured after atrial contraction just prior to the onset of systole [45, 46]. Left ventricular end-diastolic pressure (LVEDP) is often measured in the cardiac catheterization laboratory before coronary angiography to assess filling pressures. Noninvasive assessments of end-diastolic chamber volume are possible, but volume assessments rely on geometric assumptions that can be influenced by arrhythmias, changes in heart rate, localized wall motion abnormalities, and the chronic ventricular dilatation that occurs in many forms of heart failure. The passive pressure-volume relationship within a chamber, which is a reflection of the passive length-tension curve in isolated myocardium, is exponential rather than linear. This exponential property contributes to having the pressure as a surrogate for a preload-limited approach since the changes in chamber pressure to volume being greater at higher volumes compared to lower volumes. Furthermore, any myocardial and pericardial conditions (i.e., pathologies) will distort the relationship between pressure and volume. Increasing preload by giving intravenous fluids would increase preload volume, which eventually increases the end-diastolic pressures (Fig. 2.13a).

Furthermore, decreasing preload by administration of oral or intravenous diuretics would decrease the preload volume and eventually LVEDP (Fig. 2.13a). Patients with pericardial tamponade compromise the capacity of the RV to dilate to accommodate further volume, and, eventually, this inability to dilate results in decreased stroke volume (Fig. 2.13c).

■ **Table 2.1** Factors affecting pressure–volume relationship

Preload	Increases	1. Greater circulating volume
		2. Exercise
		3. Bradycardia (increased ventricular filling time)
		4. Arterioventricular fistulae
		5. Increased ventricular compliance
		6. Heart failure with reduced ejection fraction (HFrEF)
		7. Increased afterload (by increasing end-systolic volume which leads to secondary increase in ventricular preload)
		(a) Increased aortic pressure
		(b) Aortic valve stenosis and insufficiency
		(c) Pulmonary valve stenosis and insufficiency
		(d) Pulmonary hypertension
	Decreases	1. Volume depletion (hemorrhage)
		2. Tachycardia (atrial tachycardia—decreased atrial filling time)
		3. Impaired atrial contraction
		4. Decreased venous return (gravity effect)
		5. Tricuspid or mitral valve stenosis
		6. Heart failure with preserved ejection fraction (HFpEF)
		7. Decreased afterload (enhances forward flow—ejection)
Afterload	Increases	1. Elevated systemic hypertension
		2. Aortic valve disease (stenosis and insufficiency)
		3. Increased vascular resistance
		4. Pulmonary hypertension
	Decreases	1. Decreased vascular resistance (septic shock)
		2. Low blood pressure
		3. Mitral regurgitation
Myocardium	Inotropy	• Increased
	Ability of the myocardium to eject	– Increased catecholamine level
		– Inotropic medication (dopamine)
		• Decreased
		– HFrEF
		– Parasympathetic stimulation
		– Beta-blockers
	Lusitropy	• Increased
	Ability of the myocardium to relax and fill	– Increased catecholamine level
		– Beta-adrenergic agonist
		• Decreased
		– Left ventricular hypertrophy (LVH)
		– HFpEF
		– Infiltrative heart disease (amyloidosis)

Fig. 2.13 Pressure–volume (PV) loops in the physiological and pathological states. (a) PV loops in normal, increased preload, and decreased preload states. (b) PV loops in response to increased and decreased afterload. (c) PV loops in the normal state and in the patient with decreased cardiac output due to pericardial tamponade. (d) PV loops with increased and decreased inotropy. (e) PV loops in the normal state and in the patient with severe aortic stenosis. (f) PV loops in normal, acute systolic heart failure and chronic heart failure



Overall, it should be emphasized that preload is a physiological factor that encompasses more than just a single value on a pressure tracing. Preload increases with increasing circulating volume, venoconstriction, exercise, arterioventricular fistulae, increased ventricular compliance, increased ventricular filling time, and systolic heart failure. Alternatively, preload decreases with volume depletion (dehydration), decreased venous return, impaired atrial contraction, tricuspid or mitral stenosis, and decreasing ventricular compliance (■ Fig. 2.13a).

Afterload

Afterload is the force against which the heart has to pump blood into the aorta and the pulmonary artery through the aortic and pulmonic valves, respectively. Afterload is consid-

ered the stress encountered by LV myofibers as they contract against the end-diastolic volume (■ Table 2.1) (■ Fig. 2.13b). The relationship between the ventricle and its afterload is key to the concept of ventriculo-arterial coupling and can be illustrated by pressure–volume loops. During the LV ejection phase of the cardiac cycle, as ventricular volume decreases, the potential for the ventricle to develop pressure also declines. The lowest volume achieved is the end-systolic volume, at which point the stroke volume has been ejected. The aortic valve subsequently closes and the diastolic phase begins. The rise in aortic pressure, all else being equal, will correlate with a decreased stroke volume and a lower aortic pressure with an increased stroke volume and ejection fraction (EF). EF is calculated as follows: $[(EDV - ESV) / EDV] \times 100 = EF (\%)$, where EDV is end-diastolic volume and ESV is end-systolic volume. Therefore, increases in the

afterload (ESV) will cause a decrease in stroke volume and EF (■ Fig. 2.13b). For example, in an individual with aortic valvular stenosis or uncontrolled elevated blood pressures, as the afterload is increased, and if the preload (end-diastolic volume) and contractility of the ventricle (inotrope) are held constant, this will result in a smaller stroke volume and an increase in end-systolic volume, shifting the curve upward (■ Fig. 2.13).

Stroke volume is reduced as increased afterload reduces the velocity of muscle fiber shortening and the velocity by which the blood is ejected. The reduced stroke volume at the same end-diastolic volume reduces the ejection fraction. Over time, compensatory mechanisms such as ventricular wall hypertrophy will attenuate the high wall stress and improve the ventricle's ability to overcome the high afterload and increase the stroke volume, thus causing the loop to increase in width. Similarly, in patients with severe aortic valve stenosis, left ventricular emptying is impaired because of high outflow resistance caused by a reduction in the valve orifice area when it opens. This high outflow resistance results in an increase in the pressure gradient across the aortic valve during ejection, such that the peak systolic pressure within the ventricle is greatly increased (■ Fig. 2.13d). In contrast, a reduction in afterload (i.e., controlled blood pressure, vasodilators) allows the LV to eject blood with less resistance, resulting in an augmentation of the stroke volume and decreased end-systolic volume. This reduction in afterload shifts the pressure–volume loop into a compressed and wider configuration (■ Fig. 2.13b). With less blood remaining in the ventricle after the ejection phase, the ventricle will fill to a lower end-diastolic volume with the reduction of afterload. Despite this mild reduction in preload (end-diastolic volume), stroke volume shows a net increase because the reduction in end-diastolic volume is less than the reduction in end-systolic volume. Following the above equation, this will also cause a net increase in the ejection fraction.

Ventricular Contractility

Ventricular contractility represents the systolic function of the ventricles. Increasing contractility increases the velocity of fiber shortening at any given preload and afterload. This response enables the ventricle to increase the rate of pressure development and ejection velocity, which leads to an increase in stroke volume and ejection fraction and a decrease in end-systolic volume. In the PV loop diagrams, increased inotropy increases the slope, which permits the ventricle to generate more pressure at a given LV volume (■ Fig. 2.13d). Decreasing inotropy has the opposite effect—resulting in increased end-systolic volume and decreased stroke volume and ejection fraction (■ Fig. 2.13d). In patients with severe systolic heart failure, there is increased end-diastolic pressure and end-diastolic volume (■ Fig. 2.13e). Afterload reduction is considered a mainstay therapy in such situations. Intravenous or oral afterload reduction therapy is determined based on the clinical stability of the patient and cardiac output at the time of presentation.

Ventricular Compliance

Pressure–volume loops highlight the nonlinear pressure and volume relationship during diastolic filling. The instantaneous slope of the curve in the filling phase (i.e., change in pressure/change in volume) represents diastolic stiffness. This parameter is termed “elastance”; the ventricle is analogous to a spring with a stiffness that increases during contraction and decreases during relaxation. Elastance can be calculated at any point during the ventricle's diastole by calculating the gradient of the curve. Beyond a volume of approximately 140 mL (the exact volume will depend on individual heart dimensions), the chamber becomes progressively more difficult to fill, requiring a greater pressure increase to effect volume changes than earlier in diastole. A thicker, stiffer ventricle, for example, in an individual with left ventricular hypertrophy, will show a steeper gradient in the diastolic curve and, hence, a greater elastance.

Left Ventricular Remodeling and the Law of Laplace

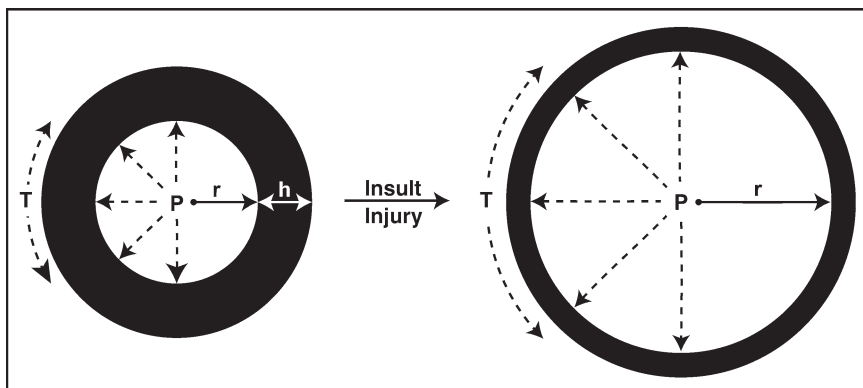
In the initial stages of failure, the heart becomes less sensitive to preload and more sensitive to afterload. The ventricular myocardial wall tension contributes to the afterload. The law of Laplace states that the wall tension is equal to the radius of the ventricular chamber multiplied by the pressure and divided by the wall thickness [$T = (P \times r)/h$] (■ Fig. 2.14). Furthermore, ventricular dilation results in increased tension associated with each myofibril, and increased wall thickness (i.e., myocardial hypertrophy) reduces afterload by distributing tension among more myofibrils. As a consequence, wall tension is greatest in the endocardial surface and is more vulnerable to reductions in coronary blood flow. While ventricular dilation initially is favorable (in order to maintain stroke volume), it brings decreased efficiency, high wall tension, and increased afterload, resulting in increased energy expenditure and deterioration of energy-starved cardiomyocytes, leading to progressive heart failure (■ Fig. 2.14).

Increasing ventricular dilation ultimately leads to valvular insufficiency, programmed cell death, and further impairment of myocardial performance. As remodeling progresses, the cellular constituents change, resulting in an increase in the non-cardiomyocyte components (including myofibroblasts, inflammatory cells, adipocytes, extracellular matrix, etc.). Therefore, effective therapies for heart failure are directed toward reverse remodeling strategies, including the use of beta-adrenergic receptor blockers, anti-fibrotic agents, and angiotensin-converting enzyme inhibitors.

Summary

In conclusion, the adult heart functions in a coordinated fashion that is highly responsive to increased stress and demand with increased cardiac output. The architectural

Fig. 2.14 Law of Laplace and cardiomyopathy. End-stage heart failure results in ventricular remodeling and chamber dilation. Based on the law of Laplace [$T = (P \times r)/h$], wall tension increases due to increased chamber dilation resulting in increased energy expenditure and progressive heart failure (T wall tension, P ventricular pressure, r radius of the chamber, h wall thickness)



organization of the heart consists of cardiomyocytes, endothelial cells, smooth muscle cells, fibroblasts, extracellular matrix, and neuronal components that collectively produce a functional syncytium. In response to a severe injury, the heart adapts in an attempt to maintain cardiac output by remodeling, which over time becomes detrimental due to a hyperadrenergic state, increased energy expenditure, increased program cell death, and progressive dilation—ultimately leading to end-stage heart failure. An enhanced understanding of the pathophysiology of the normal and failing heart allows for early implementation of conventional and emerging therapies that promote reverse remodeling of the failing heart.

References

- Harvey W. Exercitatio anatomica de motu cordis et sanguinis in animalibus. Frankfurt; 1628.
- Ringer S. A further contribution regarding the influence of the different constituents of the blood on the contraction of the heart. *J Physiol.* 1883;4(1):29–42.3.
- Reuter H, Seitz N. The dependence of calcium efflux from cardiac muscle on temperature and external ion composition. *J Physiol.* 1968;195(2):451–70.
- Kirchberger MA, Tada M, Katz AM. Phospholamban: a regulatory protein of the cardiac sarcoplasmic reticulum. *Recent Adv Stud Cardiac Struct Metab.* 1975;5:103–15.
- Tada M, Inui M. Regulation of calcium transport by the ATPase-phospholamban system. *J Mol Cell Cardiol.* 1983;15(9):565–75.
- Wiggers CJ. Studies on the consecutive phases of the cardiac cycle. I. The duration of the consecutive phases of the cardiac cycle and the criteria for their precise determination. *Am J Physiol.* 1921;56:415–38.
- Fick A. Ueber die Messung des Blutquantums in den Herzventrikeln. *Ges. Würzburg;* 1870. *SB Phys-Med.*
- Cournand A. Measurement of the cardiac output in man using the right heart catheterization. Description of technique, discussion of validity and of place in the study of the circulation. *Federation Proc.* 1945;4:207–12.
- Frank O. Zur Dynamik des Herzmuskels. *Z Biol.* 1895;32:370–437.
- Patterson SW, Piper H, Starling EH. The regulation of the heart beat. *J Physiol.* 1914;48(6):465–513.
- Sarnoff SJ, Berglund E. Ventricular function. I. Starling's law of the heart studied by means of simultaneous right and left ventricular function curves in the dog. *Circulation.* 1954;9(5):706–18.
- Sonnenblick EH. Implications of muscle mechanics in the heart. *Fed Proc.* 1962;21:975–90.
- Guyton AC, Coleman TG, Granger HJ. Circulation: overall regulation. *Annu Rev Physiol.* 1972;34:13–46.
- Braunwald E. Eugene Braunwald: escaping death and prolonging lives [part 1] Interview by Ruth Williams. *Circ Res.* 2010;106(11):1668–71.
- Opie LH. Heart physiology, from cell to circulation. 4th ed. Philadelphia, PA: Lippincott, Williams & Wilkins; 2004.
- Anderson RH, Razavi R, Taylor AM. Cardiac anatomy revisited. *J Anat.* 2004;205(3):159–77.
- Conti CR. The Netter collection of medical illustrations: cardiovascular system. 2nd ed. Philadelphia, PA: Elsevier; 2014.
- Dell'Italia LJ. Anatomy and physiology of the right ventricle. *Cardiol Clin.* 2012;30(2):167–87.
- Loukas M, Sharma A, Blaak C, Sorenson E, Mian A. The clinical anatomy of the coronary arteries. *J Cardiovasc Transl Res.* 2013;6(2):197–207.
- Benjamin MM, Smith RL, Grayburn PA. Ischemic and functional mitral regurgitation in heart failure: natural history and treatment. *Curr Cardiol Rep.* 2014;16(8):517.
- Opie LH. Mechanisms of cardiac contraction and relaxation. In: Libby P, Bonow RO, Mann DL, Zipes DP, editors. Braunwald's heart disease: a textbook of cardiovascular medicine. Chapter 21. 8th ed. Philadelphia, PA: Saunders; 2008. p. 509–39.
- Bers DM. Calcium cycling and signaling in cardiac myocytes. *Annu Rev Physiol.* 2008;70:23–49.
- Granger HJ. Cardiovascular physiology in the twentieth century: great strides and missed opportunities. *Am J Physiol.* 1998;275(6 Pt 2):H1925–36.
- Katz AM. Chapter 1, Ultrastructure of the working myocardial cell Structure of the heart and cardiac muscle. In: Physiology of the heart. 5th ed. Philadelphia, PA: Lippincott Williams and Wilkins, a Wolters Kluwer business; 2011. p. 3–32.
- Grange RW, Meeson A, Chin E, Lau KS, Stull JT, Shelton JM, Williams RS, Garry DJ. Functional and molecular adaptations in skeletal muscle of myoglobin-mutant mice. *Am J Physiol Cell Physiol.* 2001;281(5):C1487–94.
- Kendrew JC, Parrish RG, Murrack JR, Orlans ES. The species specificity of myoglobin. *Nature.* 1954;174(4438):946–9.
- Garry DJ, Kanatous SB, Mammen PP. Emerging roles for myoglobin in the heart. *Trends Cardiovasc Med.* 2003;13(3):111–6.
- Perkoff GT, Tyler FH. Estimation and physical properties of myoglobin in various species. *Metabolism.* 1958;7(6):751–9.
- Wittenberg BA, Wittenberg JB, Caldwell PR. Role of myoglobin in the oxygen supply to red skeletal muscle. *J Biol Chem.* 1975;250(23):9038–43.
- Kendrew JC, Bodo G, Dintzis HM, Parrish RG, Wyckoff H, Phillips DC. A three-dimensional model of the myoglobin molecule obtained by x-ray analysis. *Nature.* 1958;181(4610):662–6.
- Garry DJ, Bassel-Duby RS, Richardson JA, Grayson J, Neuffer PD, Williams RS. Postnatal development and plasticity of specialized muscle fiber characteristics in the hindlimb. *Dev Genet.* 1996;19(2):146–56.

32. Garry DJ, Ordway GA, Lorenz JN, Radford NB, Chin ER, Grange RW, Bassel-Duby R, Williams RS. Mice without myoglobin. *Nature*. 1998;395(6705):905–8.
33. Meeson AP, Radford N, Shelton JM, Mammen PP, DiMaio JM, Hutcheson K, Kong Y, Elterman J, Williams RS, Garry DJ. Adaptive mechanisms that preserve cardiac function in mice without myoglobin. *Circ Res*. 2001;88(7):713–20.
34. Rayment I, Holden HM, Whittaker M, Yohn CB, Lorenz M, Holmes KC, Milligan RA. Structure of the actin-myosin complex and its implications for muscle contraction. *Science*. 1993;261(5117):58–65.
35. Ginsburg KS, Weber CR, Bers DM. Cardiac Na⁺-Ca²⁺ exchanger: dynamics of Ca²⁺-dependent activation and deactivation in intact myocytes. *J Physiol*. 2013;591(8):2067–86.
36. Bers DM, Shannon TR. Calcium movements inside the sarcoplasmic reticulum of cardiac myocytes. *J Mol Cell Cardiol*. 2013;58:59–66.
37. Tada M, Katz AM. Phosphorylation of the sarcoplasmic reticulum and sarcolemma. *Annu Rev Physiol*. 1982;44:401–23.
38. Picht E, Zima AV, Shannon TR, Duncan AM, Blatter LA, Bers DM. Dynamic calcium movement inside cardiac sarcoplasmic reticulum during release. *Circ Res*. 2011;108(7):847–56.
39. Zima AV, Picht E, Bers DM, Blatter LA. Termination of cardiac Ca²⁺ sparks: role of intra-SR [Ca²⁺], release flux, and intra-SR Ca²⁺ diffusion. *Circ Res*. 2008;103(8):e105–15.
40. Suga H, Hisano R, Hirata S, Hayashi T, Ninomiya I. Mechanism of higher oxygen consumption rate: pressure-loaded vs. volume-loaded heart. *Am J Physiol*. 1982;242(6):H942–8.
41. Ross Jr J, Braunwald E. Studies on Starling's law of the heart. IX. The effects of impeding venous return on performance of the normal and failing human left ventricle. *Circulation*. 1964;30:719–27.
42. Corsi C, Lang RM, Veronesi F, Weinert L, Caiani EG, MacEneaney P, Lamberti C, Mor-Avi V. Volumetric quantification of global and regional left ventricular function from real-time three-dimensional echocardiographic images. *Circulation*. 2005;112(8):1161–70.
43. Chirinos JA, Segers P, Rietzschel ER, De Buyzere ML, Raja MW, Claessens T, De Bacquer D, St John Sutton M, Gillebert TC, Asklepios Investigators. Early and late systolic wall stress differentially relate to myocardial contraction and relaxation in middle-aged adults: the Asklepios study. *Hypertension*. 2013;61(2):296–303.
44. Wiggers C. Modern aspects of the circulation in health and disease. Philadelphia, PA: Lea & Febiger; 1915.
45. Ross Jr J, Franklin D, Sasayama S. Preload, afterload, and the role of afterload mismatch in the descending limb of cardiac function. *Eur J Cardiol*. 1976;4(Suppl):77–86.
46. Katz AM. Ernest Henry Starling, his predecessors, and the "Law of the Heart". *Circulation*. 2002;106(23):2986–92.

Congestive Heart Failure and Cardiac Transplantation

Clinical, Pathology, Imaging and Molecular Profiles

Garry, D.; Wilson, R.; Vlodaver, Z. (Eds.)

2017, XVI, 572 p. 237 illus., 141 illus. in color.,

Hardcover

ISBN: 978-3-319-44575-5